ChemComm

Cite this: *Chem. Commun.*, 2011, **47**, 6138–6140

www.rsc.org/chemcomm

COMMUNICATION

From titanium oxydifluoride ($TiOF_2$) to titania (TiO_2): phase transition and non-metal doping with enhanced photocatalytic hydrogen (H_2) evolution properties†

Ci Zhang Wen,[a] Qiu Hong Hu,[b] Ya Nan Guo,[b] Xue Qing Gong,[c] Shi Zhang Qiao*[b] and Hua Gui Yang*[a]

Received 14th February 2011, Accepted 7th April 2011
DOI: 10.1039/c1cc10851d

Single-crystalline $TiOF_2$ crystals with cubical morphology were prepared *via* a facile solvothermal method and their transformation to anatase TiO_2 under different calcination conditions such as pure argon, moist argon and pure hydrogen sulfide (H_2S) was explored by using XRD/Raman/UV-Vis/SEM/TEM/SAED. The non-metal sulfur doping was successfully fulfilled and the doped TiO_2 microcubes showed the best photocatalytic H_2 evolution property.

Considering the conventional H_2 production, which has great reliance on depleting fossil fuels and suffers from the carbon dioxide emission issue, direct splitting of water using a particulate semiconductor photocatalyst under sun light irradiation would be one of the most promising technologies to produce clean and recyclable hydrogen on a large scale in the future.[1–4] Developing highly-efficient, stable photocatalysts or photocatalytic systems always plays an important role in water cleavage processes.[5–9] Transition metal oxides with octahedrally coordinated d^0 metal ions including Ti^{4+}, Zr^{4+}, Nb^{5+}, and Ta^{5+} and some other metal oxides involving octahedrally coordinated d^{10} metal ions such as In^{3+}, Sn^{4+}, and Sb^{5+} have been reported as the candidates for water splitting.[10] As the first generation photocatalyst for H_2 evolution, TiO_2-based semiconductor material has been widely studied, which also includes the endeavours to extend the adsorption spectrum to the visible light region. Numerous efforts including crystal shape engineering, metal or non-metal doping and multi-component heterostructuring were made to enhance the photocatalytic efficiency.[4,11–15] Recently, titanium oxydifluoride ($TiOF_2$) was proposed to be an active photocatalyst and its key role in the photo-degradation of 4-chlorophenol under visible light irradiation was studied experimentally.[16] However, a pure $TiOF_2$ photocatalyst may have the issues such as low thermal stability, poor visible light adsorption, and non-ideal chemical resistance *etc*. Thus developing new photocatalysts derived from original $TiOF_2$ may overcome these disadvantages and the photocatalytic water cleavage efficiency might be also enhanced. Herein, we report a study on the transformation of $TiOF_2$ to anatase TiO_2 under different reaction conditions and sulfur doping on produced anatase TiO_2 was also fulfilled, which showed the enhanced optical and photocatalytic H_2 evolution properties.

Single-crystalline pure-phase $TiOF_2$ was synthesized *via* a simple solvothermal method using titanium(IV) tetrafluoride-(TiF_4) and 48% hydrofluoric acid (HF) solution as the precursors and *n*-butanol as the solvent (see ESI† for experimental details). ***Caution!*** *Hydrofluoric acid is extremely corrosive and it should be handled with extreme care*. The typical X-ray diffraction (XRD) patterns of the original untreated $TiOF_2$ (Fig. 1c) and the samples prepared by heat-treating original $TiOF_2$ crystals at 600 °C and 300 °C for 4 h in a moist argon atmosphere (Fig. 1a and 1b) show the evolution of crystal phases. The overall bulk crystal phase was still kept as original cubic $TiOF_2$ (space group *Pm*3*m*, JCPDS No. 08-0060) when the sample was treated at 300 °C for 4 h while phase pure anatase TiO_2 was generated if calcination temperature was increased to 600 °C.[16] Interestingly, Raman spectra of the sample prepared by heat-treating original $TiOF_2$ crystals at 300 °C show a typical tetragonal anatase TiO_2 phase instead of cubic $TiOF_2$ where strong bands at 147, 392, 519, 629 cm^{-1} were observed (Fig. 1e). All of these bands can be assigned to the anatase phase with typical Raman bands at 144 (E_g), 399 (B_{1g}), 515 (A_{1g}), 519 (B_{1g}, superimposed with the 515 cm^{-1} band), and 639 cm^{-1} (E_g).[17] This non-consistence between XRD and Raman spectra for the sample treated at 300 °C is due to the *in situ* formation of an anatase TiO_2 surface phase, which generally can only be detected by UV or visible Raman

[a] *Key Laboratory for Ultrafine Materials of Ministry of Education, School of Materials Science and Engineering, East China University of Science and Technology, 130 Meilong Road, Shanghai, 200237, China. E-mail: hgyang@ecust.edu.cn; Fax: +86 21 64252127; Tel: +86 21 64252127*
[b] *The University of Queensland, ARC Centre of Excellence for Functional Nanomaterials, Australian Institute for Bioengineering and Nanotechnology, QLD 4072, Australia. E-mail: s.qiao@uq.edu.au; Fax: +61 7 33463973; Tel: +61 7 33463815*
[c] *Labs for Advanced Materials, Research Institute of Industrial Catalysis, East China University of Science and Technology, 130 Meilong Road, Shanghai, 200237, China*

† Electronic supplementary information (ESI) available: Experimental details, TG and DSC spectra, XPS and SEM images of the transformation process under a pure argon atmosphere. See DOI: 10.1039/c1cc10851d

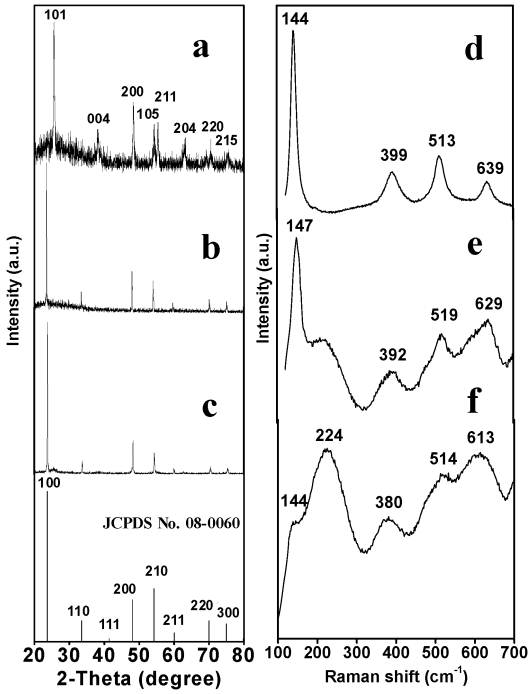

Fig. 1 XRD patterns of the anatase TiO_2 prepared by heat-treating $TiOF_2$ at 600 °C for 4 h in a moist argon atmosphere (a), $TiOF_2$ crystals with an anatase TiO_2 surface phase derived by heat-treating $TiOF_2$ at 300 °C for 4 h in a moist argon atmosphere (b), and original untreated $TiOF_2$ (c). (d)–(f) Corresponding Raman spectra of the three samples shown in (a)–(c).

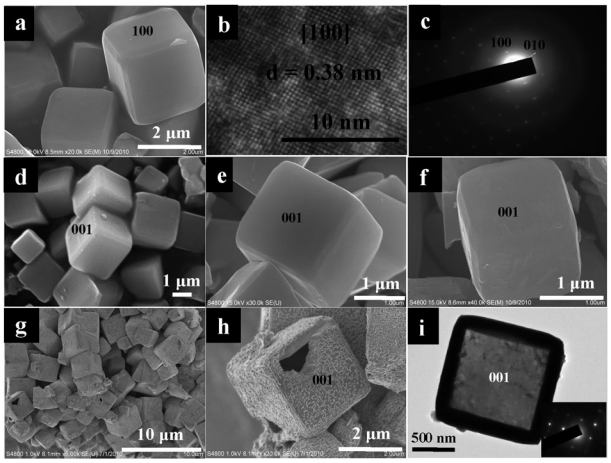

Fig. 2 (a)–(c) SEM, cross-sectional HRTEM images and SAED pattern of the as-obtained single-crystalline cubic $TiOF_2$ particles. (d) and (e) SEM images of $TiOF_2$ crystals with an anatase TiO_2 surface phase and pure anatase TiO_2 prepared through calcinating the $TiOF_2$ crystals in a moist argon atmosphere at 300 °C and 600 °C for 4 h, respectively. (f) SEM image of anatase TiO_2 prepared through calcinating the $TiOF_2$ crystals in H_2S at 800 °C for 4 h. (g) and (h) SEM images of anatase TiO_2 prepared through calcinating the $TiOF_2$ crystals in pure argon at 800 °C for 4 h. (i) TEM image and SAED pattern (the inset) of anatase TiO_2 prepared through calcinating the $TiOF_2$ crystals in pure argon at 800 °C for 4 h.

spectroscopy. Furthermore, consistent with the XRD result (Fig. 1a), the Raman spectra of the sample treated at 600 °C (Fig. 1d) illustrates a typical anatase TiO_2 phase. Based on this structural information, it can be concluded that the phase transition from cubic $TiOF_2$ to tetragonal anatase TiO_2 should start from the surface of $TiOF_2$ microcubes and then extend to the whole particles. Moreover, thermal gravimetric (TG) and differential scanning calorimeter (DSC) analysis of the as-synthesized $TiOF_2$ were also carried out, indicating that the weight loss started to occur at 300 °C and then the rate of weight loss increased significantly at 430 °C (see ESI†, Fig. S1). These results clearly illustrate a slow surface phase transition under low temperature and then a relative fast bulk phase transition under high temperature from $TiOF_2$ to anatase TiO_2. Furthermore, X-ray photoelectron spectroscopy (XPS) spectra (see ESI†, Fig. S2) not only demonstrate the typical chemical compositions and bonding states of original $TiOF_2$ and anatase TiO_2 crystals but also give the evidence on the effective sulfur doping; the S 2p core electrons with their central positions at 163.1 eV and 168.5 eV confirm the formation of sulfur doped anatase TiO_2.[18–24]

Scanning electron microscopy (SEM), cross-sectional high resolution transmission electron microscopy (HRTEM) images, and selected-area electron diffraction (SAED) pattern of the cubical $TiOF_2$ in Fig. 2a–c confirm the single crystalline characteristics and an inter-planar space of 0.38 nm between (100) planes. Due to the symmetries of the cubical $TiOF_2$ crystals, all the flat, square surfaces can be indexed into {100} facets. The single crystalline $TiOF_2$ cubes were then calcinated in moist argon, pure argon and pure H_2S at different temperatures (see ESI† for experimental details) and the corresponding SEM images are given in Fig. 2d–h. All the treated samples also exhibit a overall cubical shape and more interestingly, the internal hollow space was generated for the sample calcinated in pure argon (see Fig. 2g–i).[25] The XRD patterns (see ESI†, Fig. S3) further confirm that the products shown in Fig. 2d–h are phase-pure anatase TiO_2 crystals. The scale-like nanosheets can also be observed on the external surface of anatase TiO_2 crystals (Fig. 2g–h), which might be exposed by highly-reactive {001} facets due to the fluorine-rich $TiOF_2$ raw materials.[5] More importantly, the external surface of all the generated anatase TiO_2 microcrystals should also be highly-reactive (001) because of the existence of an F capping agent and small lattice mismatch ($\sim$0.34%) between the (100) plane of cubic $TiOF_2$ (space group $Pm3m$, a,b,c = 3.798 Å)[16,24] and the (001) plane of tetragonal anatase TiO_2 (space group $I41/amd$, a,b = 3.7852 Å and c = 9.5139 Å).[5] However, when $TiOF_2$ was treated at 900 °C under the same pure argon atmosphere, the formed anatase TiO_2 crystals have a smooth surface without {001} faceted nanosheets (Fig. S4d, ESI†) which might be due to the effective fluorine removal under high temperature. More SEM images of the products treated at different temperatures are given in Fig. S4, ESI.† The optical properties of the original untreated $TiOF_2$ and the samples calcinated under moist argon, pure argon and H_2S were monitored by UV-vis spectroscopy and the results in Fig. 3 clearly indicate that the phase transition from $TiOF_2$ to anatase TiO_2 can increase the photon adsorption in the visible light region. Sulfur doping will further enhance the visible light response.[26]

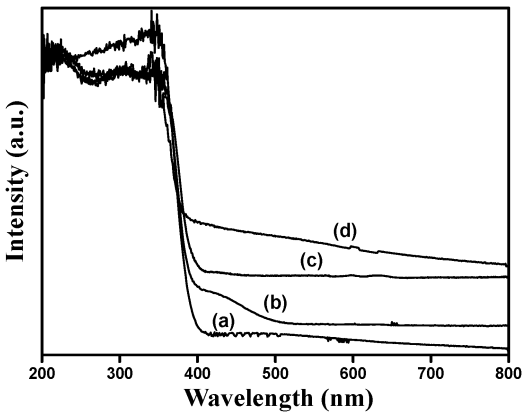

Fig. 3 (a)–(d) UV-vis spectra of original untreated $TiOF_2$ and the anatase TiO_2 prepared through calcinating the $TiOF_2$ crystals under moist argon, pure argon and H_2S, respectively.

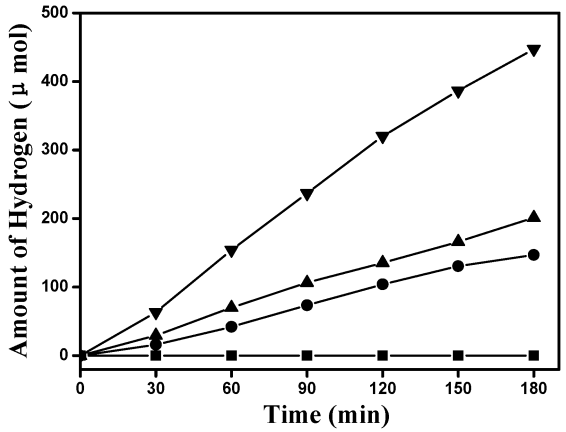

Fig. 4 The photocatalytic water splitting properties of the as-obtained $TiOF_2$ (■) and the anatase TiO_2 crystals prepared through calcinating the $TiOF_2$ crystals under moist argon (●), pure argon (▲) and H_2S (▼), respectively.

In order to study the photocatalytic properties of the original $TiOF_2$ and various derived anatase TiO_2 crystals, we then measured the efficiency of hydrogen evolution of all the samples loaded with 1 wt% Pt in the presence of methanol as a scavenger (see ESI† for the experimental details). As shown in Fig. 4, the sulfur doped anatase TiO_2 crystals have the highest photocatalytic efficiency (7054.5 μmol h^{-1} g^{-1}) and the original $TiOF_2$ did not demonstrate detectable photocatalytic activity for H_2 evolution, which matches well with the corresponding UV-vis spectra in Fig. 3.

In summary, using titanium oxydifluoride as a solid precursor, phase transition and non-metal doping were fulfilled to generate various anatase TiO_2 crystals with enhanced photocatalytic H_2 evolution properties. Single-crystalline $TiOF_2$ with cubic morphology was prepared using a simple solvothermal method and its transformation to anatase TiO_2 crystals under different calcination atmospheres such as pure argon, moist argon and pure hydrogen sulfide (H_2S) was studied systematically, which reveals that treating conditions have impact on the overall morphology, optical property and photocatalytic activity of the final products.

This work was financially supported by Scientific Research Foundation of East China University of Science and Technology (YD0142125), Pujiang Talents Programme and Major Basic Research Programme of Science and Technology Commission of Shanghai Municipality (09PJ1402800, 10JC1403200), Shuguang Talents Programme of Education Commission of Shanghai Municipality (09SG27), National Natural Science Foundation of China (20973059, 91022023, 21076076, 20703017), Fundamental Research Funds for the Central Universities (WJ0913001) and Program for New Century Excellent Talents in University (NCET-09-0347) and the Australian Research Council (ARC) through Discovery Project program (DP1095861, DP0987969).

Notes and references

1 A. Fujishima and K. Honda, *Nature*, 1972, **238**, 37.
2 M. Yoshino, M. Kakihana, W. S. Cho, H. Kato and A. Kudo, *Chem. Mater.*, 2002, **14**, 3369.
3 J. Sato, N. Saito, H. Nishiyama and Y. Inoue, *J. Phys. Chem. B*, 2003, **107**, 7965.
4 G. Liu, H. G. Yang, X. W. Wang, L. N. Cheng, J. Pan, G. Q. Lu and H. M. Cheng, *J. Am. Chem. Soc.*, 2009, **131**, 12868.
5 H. G. Yang, C. H. Sun, S. Z. Qiao, J. Zou, G. Liu, S. C. Smith, H. M. Cheng and G. Q. Lu, *Nature*, 2008, **453**, 638.
6 J. H. Park, S. Kim and A. J. Bard, *Nano Lett.*, 2006, **6**, 24.
7 J. Rossmeisl, K. Dimitrievski, P. Siegbahn and J. K. Nørskov, *J. Phys. Chem. C*, 2007, **111**, 18821.
8 S. Y. Ryu, W. Balcerski, T. K. Lee and M. R. Hoffmann, *J. Phys. Chem. C*, 2007, **111**, 18195.
9 M. Yoshida, A. Yamakata, K. Takanabe, J. Kubota, M. Osawa and K. Domen, *J. Am. Chem. Soc.*, 2009, **131**, 13218.
10 K. Ikarashi, J. Sato, H. Kobayashi, N. Saito, H. Nishiyama and Y. Inoue, *J. Phys. Chem. B*, 2002, **106**, 9048.
11 S. C. Li, L. N. Chu, X. Q. Gong and U. Diebold, *Science*, 2010, **328**, 882.
12 H. G. Yang and H. C. Zeng, *J. Phys. Chem. B*, 2004, **108**, 3492.
13 S. W. Liu, J. G. Yu and M. Jaroniec, *J. Am. Chem. Soc.*, 2010, **132**, 11914.
14 J. Yu, Q. Xiang, J. Ran and S. Mann, *CrystEngComm*, 2010, **12**, 872.
15 J. Yu, L. Qi and M. Jaroniec, *J. Phys. Chem. C*, 2010, **114**, 13118.
16 J. Zhu, D. Zhang, Z. Bian, G. Li, Y. Huo, Y. Lu and H. Li, *Chem. Commun.*, 2009, 5394.
17 T. Ohsaka, *J. Phys. Soc. Jpn.*, 1980, **48**, 1661.
18 X. W. Lou and H. C. Zeng, *J. Am. Chem. Soc.*, 2003, **125**, 2697.
19 G. Liu, C. Sun, S. C. Smith, L. Wang, G. Q. Lu and H. M. Cheng, *J. Colloid Interface Sci.*, 2010, **349**, 477.
20 E. L. D. Hebenstreit, W. Hebenstreit and U. Diebold, *Surf. Sci.*, 2001, **470**, 347.
21 T. Umebayashi, T. Yamaki, H. Itoh and K. Asai, *Appl. Phys. Lett.*, 2002, **81**, 454.
22 F. Saito, Q. Zhang and J. Kano, *J. Mater. Sci.*, 2004, **39**, 5051.
23 W. Ho, J. C. Yu and S. Lee, *J. Solid State Chem.*, 2006, **179**, 1171.
24 X. Tang and D. Li, *J. Phys. Chem. C*, 2008, **112**, 5405.
25 J. C. Lytle, H. Yan, R. T. Turgeon and A. Stein, *Chem. Mater.*, 2004, **16**, 3829.
26 G. Liu, L. Wang, H. G. Yang, H. M. Cheng and G. Q. Lu, *J. Mater. Chem.*, 2010, **20**, 831.

